

Hubbard model on bipartite lattices: zero modes and entangled spin states

Amit Gof

Hubbard model on bipartite lattices: zero modes and entangled spin states

Research Thesis

Submitted in partial fulfillment of the requirements
for the degree of Master of Science in Physics

Amit Gofit

Submitted to the Senate
of the Technion — Israel Institute of Technology
Nisan 5780 Haifa April 2020

This research was carried out under the supervision of Prof. Eric Akkermans, in the Faculty of Physics.

Acknowledgements

I would like to thank my thesis advisor Prof. Eric Akkermans for his support throughout my research and in writing my thesis, his meaningful input to my work, and for many fascinating group meetings and conversations during lunch breaks.

The generous financial help of the Technion is gratefully acknowledged.

Contents

List of Figures

Abstract	1
1 Introduction	3
1.1 Bipartite lattices	3
1.2 Hubbard model	4
1.3 Vacancies	5
1.4 Graphene	6
2 Spin in the ground state of bipartite lattices	7
2.1 Properties of bipartite lattices	7
2.2 Spin Operators	10
2.3 Symmetries of the Hubbard model on a bipartite lattice	10
2.4 A theorem by Lieb	12
2.5 Vacancies on a bipartite lattice	13
2.6 Hubbard interaction as a perturbation	13
2.6.1 No interaction	13
2.6.2 Perturbation theory	14
2.7 First order perturbation theory	17
2.8 Graphene as an example of a Hubbard model on a bipartite lattice - effect of vacancies	20
2.9 Entangled spin states	20
2.10 Connection to topology	21
3 Conclusion and open questions for fututre work	25
A Appendix	27
A.1 Creation and annihilation operators transformations	27
A.1.1 Base transformation	27
A.1.2 Spin operators	28
A.1.3 Symmetries	28
A.2 The effective Hamiltonian	29

List of Figures

1.1	Examples of lattices. Only lattice (3) satisfies the definition of a bipartite lattice, where the orange and green sites represent respectively the two sublattices.	3
1.2	Examples of bipartite lattices. From left to right: a two dimensional cubic lattice and the honeycomb lattice both with nearest neighbor interactions. The orange and green sites depicts respectively two sublattices.	4
1.3	Vacancies in a bipartite lattice. The orange and green sites are defined as in Fig. 1.2. The white empty circles represent vacancies, i.e., the removal of a site, and hence of a neutral atom from the lattice.	5
1.4	Graphene honeycomb lattice.	6
2.1	A qualitative example of a symmetric and gapped spectrum around zero energy.	8
2.2	The spectrum of graphene in the tight binding approximation. The spectrum is linear near the Dirac points ($E \propto \pm k $) and therefore symmetric around zero energy. There are six Dirac points that are divided into two equivalence sets of three points. One can look at one of the Dirac points only since the other one will only give a degeneracy that will not affect any charge or spin related properties. Taken from https://pages.shanti.virginia.edu/mirzamonzur/research/ (the Fig. was altered from the original).	9
2.3	Three examples of filling the energy levels in the ground state of H_0 with 3 vacancies on the same sublattice, e.g., $N = 10$ sites, 3 vacancies leads to 7 spin 1/2 fermions at half filling. Example (2) is a state with maximal spin, and it is also the ground state when a Hubbard interaction is added (Section 2.7).	14
2.4	A spatially localized zero mode on a vacancy in graphene. The blue dots represent the strength of the square of the wave function of the zero modes (taken from [Ovdat et al., 2018]).	21

2.5	Measurement of the local density of states as a function of voltage (that can be converted to spectral energy) with and without vacancy. The sharp peak at zero energy (Fermi energy) corresponds to the expected zero mode localized on the vacancy (taken from [Ugeda et al., 2010], the figure was altered from the original).	22
2.6	An example with two types of vacancies, each color (green or purple) represent a vacancy on a different sublattice. There are two green vacancies and one purple vacancy. A local fractional charge, which is proportional to zero mode wave function squared, (blue dots) is formed around the type of vacancies whose number is larger, in this case the green vacancies.	23
2.7	A spatially localized spin (blue dots) is formed around the vacancy. The red arrow represents the total spin in the z direction, which in this example is up.	23
2.8	An example of a spin entangled state in graphene. The blue dots and red arrows are defined as in Fig. 2.7. In this example the total spin is $S = 1$ (from equation (2.36)), since there are two green vacancies and zero purple vacancies. Thus an entangled state $ \psi\rangle = \frac{1}{\sqrt{2}} (\uparrow\downarrow\rangle + \downarrow\uparrow\rangle)$ of two electrons on two distant vacancies can be created.	24

Abstract

This thesis is devoted to a study of the total spin in the ground state of spin $1/2$ fermions described by a Hubbard model defined on bipartite lattices with vacancies. Bipartite lattices are defined as direct sums of two sub lattices A and B so that each site is connected only to sites of the other sub lattice. The spectrum of single particle Hamiltonians on such lattices display a symmetry between positive and negative energies and it may host zero energy states. A vacancy defined by the removal of a single site, can be either of type A or B . An important result of Lieb (1989) determines the ground state spin of the Hubbard model on a bipartite lattice with a finite number of sites, without vacancies and for arbitrary Hubbard interactions.

Using first order perturbation theory, i.e. for weak on-site interactions, we have found that in the presence of a finite number of vacancies V_A and V_B , the ground state retains a finite spin given by $S = \frac{1}{2}|V_A - V_B|$. This result is independent of the number of lattice sites (either finite or infinite) and it is a consequence of vacancy-induced zero modes. These zero modes define a subspace of the total Hilbert space which stays invariant against Hubbard interactions. This robustness is a consequence of topological properties of bipartite lattices not anticipated in the literature. We build on this topological protection of the ground state spin to speculate on the generalisation of our result beyond perturbation theory and to predict interesting properties of spatially remote entangled spin states. Graphene is a natural platform for these ideas and it may be used to give them interesting applications.

Chapter 1

Introduction

1.1 Bipartite lattices

A lattice is a collection of sites connected to each other by bonds. A lattice is bipartite if its sites can be divided into two sublattices where sites in one sublattice only interacts with sites in the other sublattice, e.g., a d dimensions cubic lattice with nearest neighbor interactions or graphene with nearest neighbor interactions (e.g., Figs. 1.1 and 1.2). One can also think of some long range interaction with specific exclusion rules that would also allow the lattice to be bipartite.

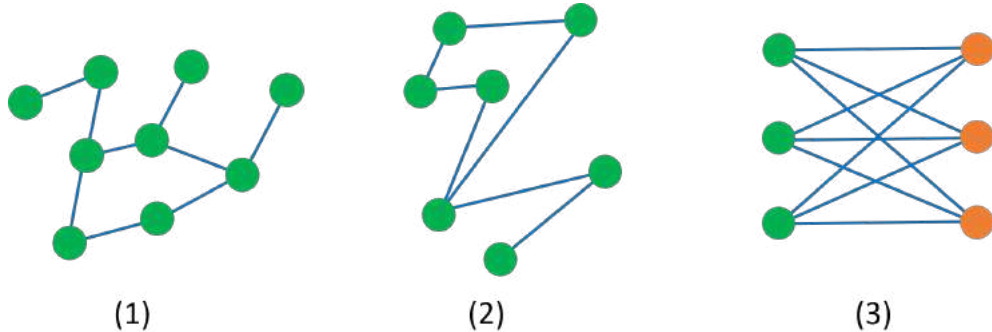


Figure 1.1: Examples of lattices. Only lattice (3) satisfies the definition of a bipartite lattice, where the orange and green sites represent respectively the two sublattices.

We denote A and B the partition into two sublattices and by N_A and N_B the respective (finite) number of sites. The adjacency matrix $A = \{a_{i,j}\}$ is defined as $a_{i,j} = 1$ if i, j are connected and $a_{i,j} = 0$ otherwise. For a bipartite lattice A is of the form

$$A = \begin{pmatrix} 0 & D \\ D^\dagger & 0 \end{pmatrix}, \quad (1.1)$$

where D is an $N_A \times N_B$ matrix. Using a tight binding description for free particles (e.g

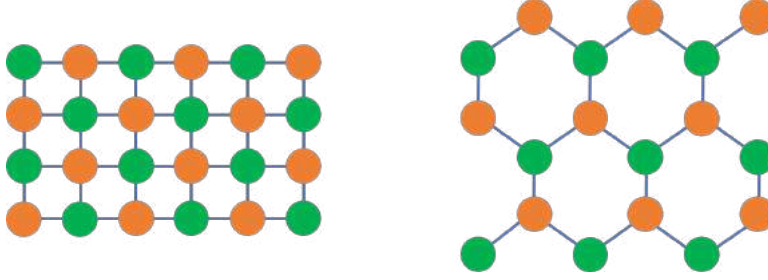


Figure 1.2: Examples of bipartite lattices. From left to right: a two dimensional cubic lattice and the honeycomb lattice both with nearest neighbor interactions. The orange and green sites depicts respectively two sublattices.

fermions) on a bipartite lattice the corresponding Hamiltonian is:

$$H_0 = \sum_{\sigma} \sum_{\langle xy \rangle} t_{xy} c_{x\sigma}^{\dagger} c_{y\sigma} \quad (1.2)$$

where $\langle \rangle$ denotes nearest neighbors, t_{ij} is a real valued symmetric matrix and $c_{x\sigma}^{\dagger}$ ($c_{x\sigma}$) are creation (annihilation) fermionic operators at site x with spin σ and satisfy $\{c_{x\sigma}, c_{y\tau}^{\dagger}\} = \delta_{xy}\delta_{\sigma\tau}$. Assuming (for simplicity) that $t_{ij} = t$, H_0 coincides with the adjacency matrix A up to the constant t .

The spectrum of H_0 on a bipartite lattice is symmetric around zero energy, and its number of zero modes is at least $|N_A - N_B|$. These zero modes rise from the nontrivial topological structure of the lattice and have unusual properties, e.g., [Brouwer et al., 2002] showed that zero modes in the random hopping model can be highly localized or highly nonlocalized depending on the boundary conditions. The number of zero modes can be extensive i.e. comparable to the (finite) number of lattice sites and gives rise to a flat band, i.e., a band of states with the same energy and no dispersion, that can result in ferromagnetic states [Mielke, 1991b, Lieb, 1989]. We will elaborate on flat bands in the context of vacancies in the Hubbard model (Section 2.5).

These properties are very general, they apply to different systems (e.g., graphene, silicene, etc.) and lead to interesting phenomena, e.g., flat bands in silicene [Hatsugai et al., 2015]. These flat bands have been extended to analogue systems, e.g., photonic zero modes [Iadecola et al., 2016].

1.2 Hubbard model

An important, yet unsolved problem in the quantum description of fermions moving in a solid is the existence and origin of a stable magnetic order. A consensual framework to answer this question is the Hubbard model described by the Hamiltonian,

$$H \equiv H_0 + H_i = H_0 + u \sum_x n_{x\uparrow} n_{x\downarrow}, \quad (1.3)$$

where $n_{x\sigma} \equiv c_{x\sigma}^\dagger c_{x\sigma}$ is the fermion number operator. The interaction term characterised by the positive and constant (to simplify) u accounts for the screened Coulomb on site repulsion. Despite being oversimplified, the Hubbard Hamiltonian displays almost all interesting observed phenomena : magnetic ordering of any kind, metal-insulator transition, superconductivity, Tomonaga-Luttinger liquid in one space dimension, and more. The Hubbard model can thus be viewed as the simplest possible model of correlated fermions with few independent parameters, the hopping t and the interaction u energies (more precisely their ratio), the particle density and the nature of the lattice, an essential property central to this thesis. The bosonic version of the Hubbard model displays also a very rich phenomenology. Despite its simplicity, only few properties of this model have been rigorously proven.

A surprising aspect is that both on-site Coulomb repulsion H_i and hopping H_0 are spin-independent hence do not favor magnetic ordering. But their sum gives rise to a variety of exotic magnetic orders of quantum origin. ([Lieb and Mattis, 1962a, Lieb and Mattis, 1962b, Nagaoka, 1966, Mielke, 1991a, Mielke, 1991b, Mielke, 1992, Mielke and Tasaki, 1993]).

For a bipartite lattice $t_{xy} = 0$ if x and y belong to the same sub-lattice. The spin of the non-degenerate ground state of the repulsive ($u > 0$) Hubbard model on a bipartite lattice where the number of electrons equals the number of sites, i.e. half filling, is $S = \frac{|N_A - N_B|}{2}$ ([Lieb, 1989]). Further more, there is a ferrimagnetic long range order for some bipartite lattices [Shen et al., 1994].

1.3 Vacancies

A vacancy is obtained by the removal of site, i.e., a neutral atom from the lattice. A vacancy can be created on a finite or an infinite lattice. The creation of vacancies on an infinite bipartite lattice has some interesting consequences, and we will discuss some of them in the next chapter (Chapter 2).

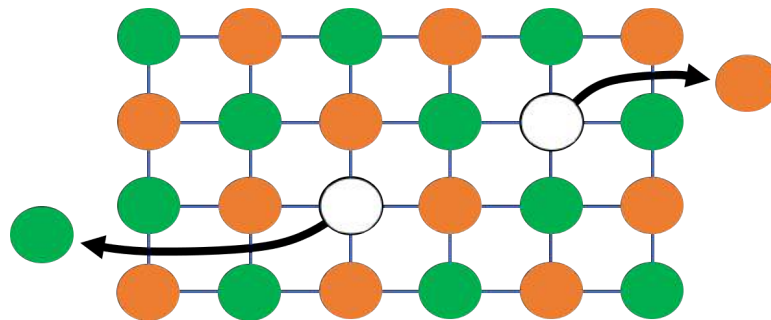


Figure 1.3: Vacancies in a bipartite lattice. The orange and green sites are defined as in Fig. 1.2. The white empty circles represent vacancies, i.e., the removal of a site, and hence of a neutral atom from the lattice.

1.4 Graphene

Graphene, a two dimensional system made of carbon atoms in a honeycomb lattice (see Fig. 1.4), has many interesting properties. It is a bipartite lattice and has a low energy spectrum, well approximated by a continuum massless Dirac fermions field. Vacancies in graphene break the sublattice symmetry, leading to the appearance of zero modes that are spatially localized on the vacancies and induce magnetism. ([Lieb, 1989, Sutherland, 1986, Pereira et al., 2007, Nanda et al., 2012, Liu et al., 2015, Mao et al., 2016, Yazyev and Helm, 2007, Palacios et al., 2008, Ulybyshev and Katsnelson, 2015, Charlebois et al., 2015]). Moreover, a local fractional charge is formed around vacancies ([Ovdat et al., 2018]). A very useful way to mimic the effect of vacancies in graphene is done by spating Hydrogen atoms on the graphene lattice as done by [González-Herrero et al., 2016]. The Hydrogen atoms bound to the Carbon atoms and effectively neutralizes them. This method is very useful since it allows to use scanning tunneling microscopy to move the Hydrogen atoms and affect the vacancies locations. Graphene is also a useful material for the study of quantum information and entangled states [Kindermann, 2009]. Silicene, the silicon equivalent of graphene, is also a potential candidate to show some of these interesting phenomena [Vogt et al., 2012].

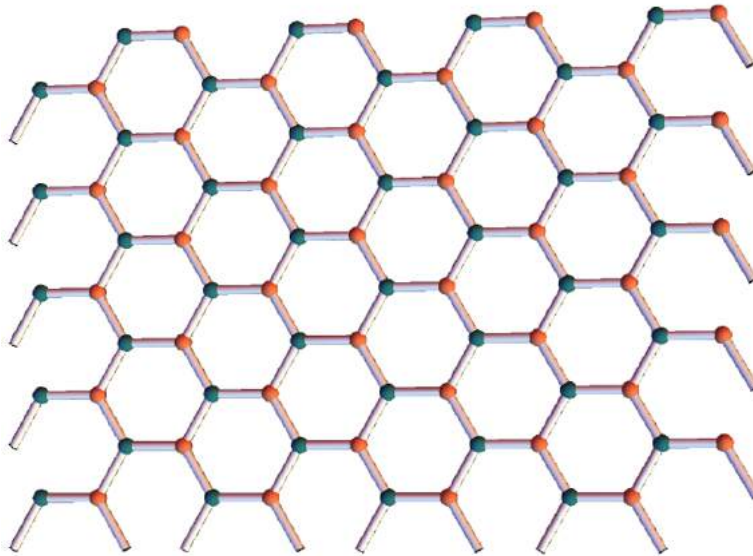


Figure 1.4: Graphene honeycomb lattice.

Chapter 2

Spin in the ground state of bipartite lattices

In this chapter we will present some properties and symmetries of the Hubbard model on bipartite lattices. We will then use these properties and symmetries to find the ground state of the Hubbard model on a bipartite lattice, and on graphene in particular, in first order perturbation theory in the Hubbard interaction and show the affect of vacancies on it. We will then show that the spin of the ground state could be entangled and try to link our results to the topology of the lattice.

2.1 Properties of bipartite lattices

Consider a bipartite lattice. From now on no further assumptions are needed. Since the lattice is bipartite, we can divide it into two sublattices, denoted A and B with respective and finite number of sites N_A and N_B . The adjacency matrix of a bipartite lattice is given by equation (1.1).

A single particle quantum Hamiltonian describing free particles on a bipartite lattice is the adjacency matrix up to a constant t $H_0 = tA$.

Thus, the most general form of the Hamiltonian must be

$$H_0 = t \begin{pmatrix} 0 & D \\ D^\dagger & 0 \end{pmatrix} \quad (2.1)$$

where D is an $N_A \times N_B$ matrix. H is an $N \times N$ matrix where $N = N_A + N_B$, This Hamiltonian has a number of interesting properties.

Define

$$\sigma_3 \equiv \begin{pmatrix} \mathbb{1}_{N_A \times N_A} & 0 \\ 0 & -\mathbb{1}_{N_B \times N_B} \end{pmatrix} \quad (2.2)$$

Note that

$$H_0\sigma_3 = t \begin{pmatrix} 0 & D \\ D^\dagger & 0 \end{pmatrix} \begin{pmatrix} \mathbb{1}_{N_A \times N_A} & 0 \\ 0 & -\mathbb{1}_{N_B \times N_B} \end{pmatrix} = t \begin{pmatrix} 0 & -D \\ D^\dagger & 0 \end{pmatrix} \quad (2.3)$$

$$\sigma_3 H_0 = \begin{pmatrix} \mathbb{1}_{N_A \times N_A} & 0 \\ 0 & -\mathbb{1}_{N_B \times N_B} \end{pmatrix} t \begin{pmatrix} 0 & D \\ D^\dagger & 0 \end{pmatrix} = t \begin{pmatrix} 0 & D \\ -D^\dagger & 0 \end{pmatrix} \quad (2.4)$$

Thus,

$$\{H_0, \sigma_3\} = 0 \quad (2.5)$$

Now assume $|\psi\rangle$ is an eigenstate of H with energy E i.e. $H|\psi\rangle = E|\psi\rangle$ Then,

$$H(\sigma_3|\psi\rangle) = -\sigma_3 H|\psi\rangle = -\sigma_3 E|\psi\rangle = -E(\sigma_3|\psi\rangle). \quad (2.6)$$

$\sigma_3|\psi\rangle$ is thus also an eigenstate of H with energy $-E$. Thus, the spectrum of a Hamiltonian on a bipartite lattice is symmetric around zero energy. (see Figs. 2.1 and 2.2).

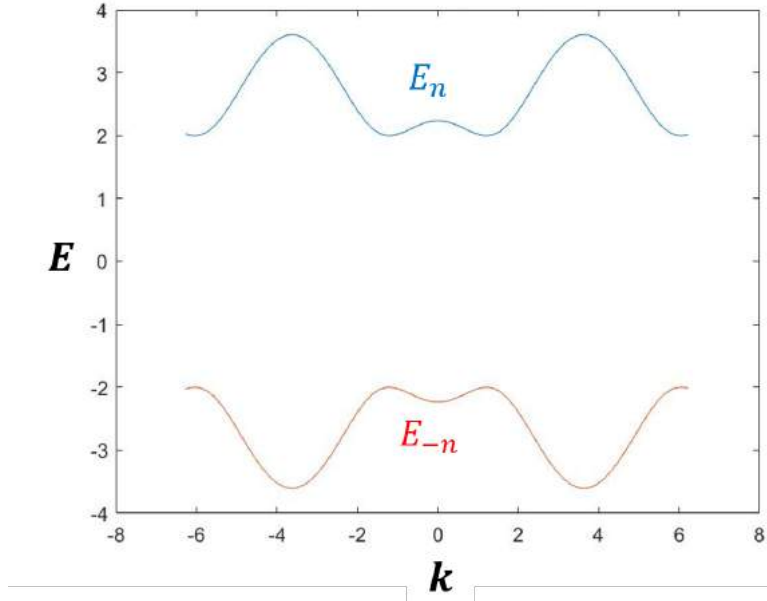


Figure 2.1: A qualitative example of a symmetric and gapped spectrum around zero energy.

Moreover, for $|\psi\rangle = \begin{pmatrix} |\psi_A\rangle \\ |\psi_B\rangle \end{pmatrix}$, $\sigma_3|\psi\rangle = \begin{pmatrix} |\psi_A\rangle \\ -|\psi_B\rangle \end{pmatrix}$. Next we wish to look for zero modes for H_0 , i.e. states that satisfy $H_0|\psi\rangle = 0$. Namely,

$$\begin{pmatrix} 0 & D \\ D^\dagger & 0 \end{pmatrix} \begin{pmatrix} |\psi_A\rangle \\ |\psi_B\rangle \end{pmatrix} = 0. \quad (2.7)$$

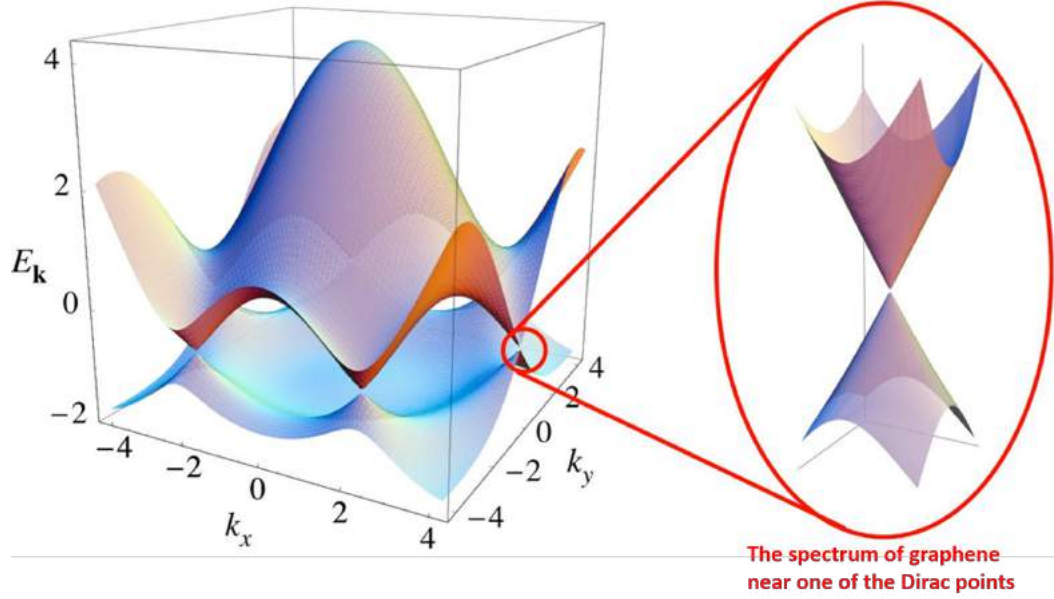


Figure 2.2: The spectrum of graphene in the tight binding approximation. The spectrum is linear near the Dirac points ($E \propto \pm|k|$) and therefore symmetric around zero energy. There are six Dirac points that are divided into two equivalence sets of three points. One can look at one of the Dirac points only since the other one will only give a degeneracy that will not affect any charge or spin related properties. Taken from <https://pages.shanti.virginia.edu/mirzamonzur/research/> (the Fig. was altered from the original).

We thus obtain two sets of equations

$$D |\psi_B\rangle = 0, D^\dagger |\psi_A\rangle = 0. \quad (2.8)$$

The first (second) set contains N_A (N_B) equations with N_B (N_A) unknowns. Assuming $N_A > N_B$, the first set is over constrained and thus the only solution is the trivial one $|\psi_B\rangle = 0$. The second set is under constrained so that there will be $N_A - N_B$ free parameters and thus $N_A - N_B$ solutions to the equation $D^\dagger |\psi_A\rangle = 0$. Hence, we expect at least $N_A - N_B$ zero modes of the form $\begin{pmatrix} |\psi_A\rangle \\ 0 \end{pmatrix}$. For $N_B > N_A$, there are $N_B - N_A$ zero modes of the form $\begin{pmatrix} 0 \\ |\psi_B\rangle \end{pmatrix}$. Finally the number of zero modes is at least $|N_A - N_B|$. This number is the index of the Hamiltonian defined as

$$\text{Index}H = \text{Dim}[\text{Ker}(D^\dagger)] - \text{Dim}[\text{Ker}(D)]. \quad (2.9)$$

Recall that the Ker of an operator is the set of states for which the operator sends to the zero state. For a finite lattice this result is obvious. It is also valid for an infinite graphene lattice as shown by [Ovdat et al., 2018]. This index satisfies the conditions in

Atiyah Singer index theorem and so it is a topological index.

2.2 Spin Operators

Consider spin 1/2 fermions (e.g., electrons) on a bipartite lattice. The spin operators are defined as

$$S^z = \frac{1}{2} \sum_x (n_{x\uparrow} - n_{x\downarrow}), \quad S^+ = (S^-)^\dagger = \sum_x c_{x\uparrow}^\dagger c_{x\downarrow}. \quad (2.10)$$

The total spin operator is given by

$$S^2 = (S^z)^2 + \frac{1}{2} (S^+ S^- + S^- S^+), \quad (2.11)$$

and has eigenvalues $S(S+1)$.

2.3 Symmetries of the Hubbard model on a bipartite lattice

We now consider again the Hubbard model on a bipartite lattice. The number of sites is $N = N_A + N_B$ and we assume the system is at half filling ($N = N_e$), where each atom contributes one conducting electron. Namely,

$$H_0 = \sum_{\sigma xy} t_{xy} c_{x\sigma}^\dagger c_{y\sigma} \quad (2.12)$$

$$U = u \sum_x n_{x\uparrow} n_{x\downarrow}. \quad (2.13)$$

$u > 0$ and $t_{xy} = 0$ if x and y belong to the same sub-lattice. The total number operators are defined as

$$N_\sigma = \sum_x n_{x\sigma}, \quad (2.14)$$

with eigenvalues $N_{e,\sigma}$. The spin operators and the total number operators commute with the Hamiltonian and therefore are good quantum numbers. H_0 anti commutes with σ_3 . This symmetry is generated by taking

$$c_{x\sigma} \rightarrow \epsilon(x) c_{x\sigma}, \quad (2.15)$$

where $\epsilon(x)$ is $+1(-1)$ if $x \in A(B)$. This is easily seen by looking at a generic term in H_0 ,

$$t_{xy} c_{x\sigma}^\dagger c_{y\sigma} \rightarrow \epsilon(x) \epsilon(y) t_{xy} c_{x\sigma}^\dagger c_{y\sigma}. \quad (2.16)$$

Since this term is nonzero only if x and y belong to different sublattices, $\epsilon(x)\epsilon(y)$ must have different signs, then

$$t_{xy}c_{x\sigma}^\dagger c_{y\sigma} \rightarrow -t_{xy}c_{x\sigma}^\dagger c_{y\sigma}, \quad (2.17)$$

and therefore $H_0 \rightarrow -H_0$. The Hubbard model for fermions however has an additional particle hole symmetry. Take

$$c_{x\sigma} \rightarrow c_{x\sigma}^\dagger, \quad (2.18)$$

a generic term in H_0 then transforms according to

$$t_{xy}c_{x\sigma}^\dagger c_{y\sigma} \rightarrow t_{xy}c_{x\sigma}c_{y\sigma}^\dagger. \quad (2.19)$$

Since this term is nonzero only if x and y belong to different sublattices than $c_{x\sigma}$ and $c_{y\sigma}^\dagger$ anticommute. Moreover t_{xy} is a symmetric matrix, so that

$$t_{xy}c_{x\sigma}^\dagger c_{y\sigma} \rightarrow t_{xy}c_{x\sigma}c_{y\sigma}^\dagger = -t_{xy}c_{y\sigma}^\dagger c_{x\sigma} = -t_{yx}c_{y\sigma}^\dagger c_{x\sigma}. \quad (2.20)$$

When we sum over x, y we obtain:

$$\sum_{xy} t_{xy}c_{x\sigma}^\dagger c_{y\sigma} \rightarrow \sum_{xy} -t_{yx}c_{y\sigma}^\dagger c_{x\sigma} = -\sum_{xy} t_{xy}c_{x\sigma}^\dagger c_{y\sigma}. \quad (2.21)$$

Note that H_0 is spin independent, hence the transformation can be done on one of the spins or both of them. By performing it on both, we obtain that $H_0 \rightarrow -H_0$. This implies we can implement the transformation

$$c_{x\sigma} \rightarrow \epsilon(x)c_{x\sigma}^\dagger, \quad (2.22)$$

for one of the spins or both of them, and deduce that $H_0 \rightarrow H_0$. Physically this transformation means that we can create a particle with energy E or destroy a particle with energy $-E$ at the same energy cost. This will be shown later. Note that under a σ_3 transformation U remains invariant:

$$U = u \sum_x n_{x\uparrow}n_{x\downarrow} = u \sum_x c_{x\uparrow}^\dagger c_{x\uparrow} c_{x\downarrow}^\dagger c_{x\downarrow} \rightarrow u \sum_x (\epsilon(x))^4 c_{x\uparrow}^\dagger c_{x\uparrow} c_{x\downarrow}^\dagger c_{x\downarrow} = U, \quad (2.23)$$

where the last equality results from the fact that $(\epsilon(x))^2 = 1$ for all x . Moreover, under a particle hole transformation we obtain

$$n_{x\sigma} = c_{x\sigma}^\dagger c_{x\sigma} \rightarrow c_{x\sigma}c_{x\sigma}^\dagger = 1 - c_{x\sigma}^\dagger c_{x\sigma} = 1 - n_{x\sigma}, \quad (2.24)$$

so that U is also invariant under particle-hole transformations:

$$U = u \sum_x n_{x\uparrow}n_{x\downarrow} \rightarrow u \sum_x (1 - n_{x\uparrow})(1 - n_{x\downarrow}) = u \sum_x (1 - N_x) + U, \quad (2.25)$$

where $N_x = n_{x\uparrow} + n_{x\downarrow}$. Note that

$$\sum_x (1 - N_x) = N - N_e. \quad (2.26)$$

At half filling we have $N = N_e$ and thus U is invariant under the transformation (2.22), and the symmetry represented by this transformation is not broken. Next we show that the total spin operator is also invariant under the transformations in equations (2.15) and (2.18). For σ_3 it is obvious since the spin operators in equation (2.10) are quadratic in creation or annihilation operators on each site, so under σ_3 we always obtain a factor of $(\epsilon(x))^2 = 1$. Under a particle-hole transformation we obtain

$$\begin{aligned} S^z &= \frac{1}{2} \sum_x (n_{x,\uparrow} - n_{x,\downarrow}) \\ &\rightarrow \frac{1}{2} \sum_x ((1 - n_{x,\uparrow}) - (1 - n_{x,\downarrow})) = -\frac{1}{2} \sum_x (n_{x,\uparrow} - n_{x,\downarrow}) = -S^z, \end{aligned} \quad (2.27)$$

$$S^+ = \sum_x c_{x\uparrow}^\dagger c_{x\downarrow} \rightarrow \sum_x c_{x\uparrow} c_{x\downarrow}^\dagger = S^-. \quad (2.28)$$

The total spin is also invariant under the transformation (2.22):

$$\begin{aligned} S^2 &= (S^z)^2 + \frac{1}{2} (S^+ S^- + S^- S^+) \\ &\rightarrow (-S^z)^2 + \frac{1}{2} (S^- S^+ + S^+ S^-) = (S^z)^2 + \frac{1}{2} (S^+ S^- + S^- S^+) = S^2. \end{aligned} \quad (2.29)$$

2.4 A theorem by Lieb

[Lieb, 1989] has proven that the ground state of $H = H_0 + U$ at half filling and even number of sites is non-degenerate, up to the usual $SU(2)$ degeneracy, and it has a finite spin of

$$S = \frac{|N_A - N_B|}{2}. \quad (2.30)$$

The fact that this is the spin value is not surprising. In the $u = 0$ limit the ground state is obtained by doubly occupying all the negative energy states and half the zero modes. The ground state is therefore degenerate but among these states there are some with maximal spin (2.30). Additionally in the large u limit using second order perturbation theory in t/u the Heisenberg model is obtained (see [Anderson, 1959]), where the ground state spin is unique and its value is 2.30. (see [Lieb and Mattis, 1962a]). In his proof, [Lieb, 1989] first shows that the ground state of the Hubbard model is unique for any $u > 0$ using the symmetries mentioned above. He then use continuity argument in u to say that the spin of the ground state is the same for all u , and in particular it is the one obtained in the large u limit, the Heisenberg limit, and so the value of the spin is 2.30.

This finite spin indicates a ferromagnetic order. This is a surprising result as there

is no magnetic order in one dimension [Lieb and Mattis, 1962b].

2.5 Vacancies on a bipartite lattice

We now wish to prove that vacancies on a bipartite lattice lead to the existence of zero modes. They also modify the ground state and its total spin. We show that by creating V_A (V_B) vacancies on sublattice A (B), the spin of the ground state of the repulsive ($u > 0$) Hubbard model on a bipartite lattice at half filling is $S = \frac{|V_A - V_B|}{2}$. We also show that the only contribution to the spin density is from the zero modes.

Assuming we can create a vacancy in a bipartite lattice without breaking the σ_3 symmetry we can change the number of sites on a finite lattice and influence the quantity $|N_A - N_B|$. This implies we can create or destroy zero modes. If we have a finite bipartite lattice with $N_A = N_B$ and create V_A (V_B) the difference between the number of sites will be $|N_A - N_B| = |V_A - V_B|$. We assume that we can work with an infinite bipartite lattice with $N_A = N_B \rightarrow \infty$. We claim that the creation of vacancies allows us to treat the lattice as a finite bipartite lattice, where $|N_A - N_B|$ is replaced with $|V_A - V_B|$. This is a very non-trivial statement as in principal, creating a vacancy on an infinite lattice does not change the number of sites. However this was proven for graphene by [Ovdat et al., 2018] at the continuum limit using the low energy Dirac limit and nontrivial chiral boundary conditions. [Ovdat et al., 2018] also showed that the number of zero modes N_{ZM} is a topological index using Atiyah–Singer index theorem and it is given by:

$$N_{ZM} = |V_A - V_B|. \quad (2.31)$$

We can create as many vacancies as we want and increase the number of zero modes, and so a flat band of zero modes can be created.

2.6 Hubbard interaction as a perturbation

2.6.1 No interaction

We first consider the $u = 0$ case:

$$H_0 = \sum_{\sigma xy} t_{xy} c_{x\sigma}^\dagger c_{y\sigma} \quad (2.32)$$

and start with an infinite lattice with $N_A = N_B$ and half filling and create V_A (V_B) vacancies of type A (B). Hence the number of zero modes is, as shown previously:

$$N_{ZM} = |V_A - V_B| \times 2, \quad (2.33)$$

where the factor 2 comes from the additional degree of freedom of the spin. Since the system is at half filling the ground state of the Hamiltonian is such that all the negative

energy states and half the zero modes are filled. Thus, the ground state is degenerate (see Fig. 2.3), and the degeneracy is:

$$\frac{(|V_A - V_B| \times 2)!}{(|V_A - V_B|!)^2} \quad (2.34)$$

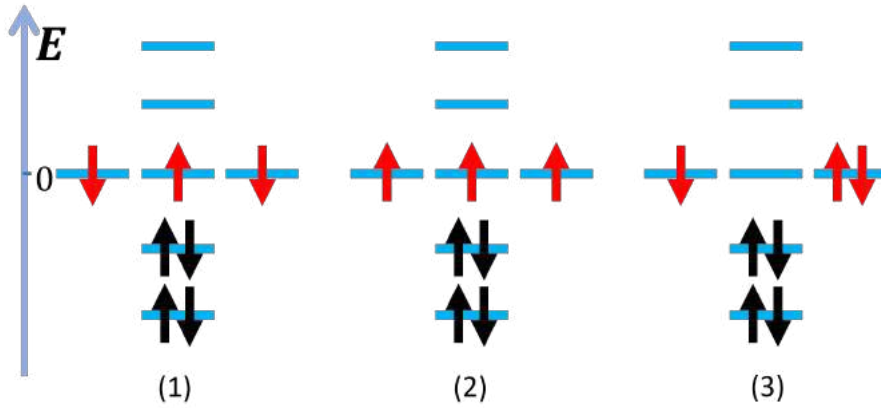


Figure 2.3: Three examples of filling the energy levels in the ground state of H_0 with 3 vacancies on the same sublattice, e.g., $N = 10$ sites, 3 vacancies leads to 7 spin 1/2 fermions at half filling. Example (2) is a state with maximal spin, and it is also the ground state when a Hubbard interaction is added (Section 2.7).

2.6.2 Perturbation theory

Adding a small $u \ll t$ Hubbard interaction

$$u \sum_x n_{x\uparrow} n_{x\downarrow}, \quad (2.35)$$

with $u > 0$, allows to treat the interaction perturbatively. From [Lieb, 1989] it is clear that a finite lattice with $|N_A - N_B| = |V_A - V_B|$ that is an even number, satisfies Lieb's theorem so that the total spin in the ground state is:

$$S = \frac{|V_A - V_B|}{2}. \quad (2.36)$$

We claim that this result remains true for an infinite lattice as well. To show it, we wish to find the ground state of the system using perturbation theory. Adding the interaction (2.35), the degeneracy in equation (2.34) is lifted (at least partially). Consider the

unitary transformation W from the position (x) to the energy representation:

$$\begin{aligned} |n_1, \sigma_1\rangle \otimes |n_2, \sigma_2\rangle \otimes \cdots \otimes |n_k, \sigma_k\rangle &= W |x_1, \sigma_1\rangle \otimes |x_2, \sigma_2\rangle \otimes \cdots \otimes |x_k, \sigma_k\rangle \\ &= \sum_{x_1, x_2, \dots, x_k} W_{n_1, n_2, \dots, n_k, x_1, x_2, \dots, x_k} |x_1, \sigma_1\rangle \otimes |x_2, \sigma_2\rangle \otimes \cdots \otimes |x_k, \sigma_k\rangle. \end{aligned} \quad (2.37)$$

It is important to note that:

$$W |0\rangle = |0\rangle, \quad (2.38)$$

a relation that will prove useful later. We define creation and annihilation operators of a spin σ particle in the energy level n ,

$$c_{n\sigma}^\dagger |0\rangle = |n, \sigma\rangle. \quad (2.39)$$

The creation and annihilation operators transform as (see the derivation in (A.1)):

$$c_{n\sigma}^\dagger = W c_{x\sigma}^\dagger W^\dagger, \quad (2.40)$$

$$c_{n\sigma} = W c_{x\sigma} W^\dagger, \quad (2.41)$$

which for practical purposes, we rewrite as

$$c_{n\sigma}^\dagger = \sum_x \psi_n(x) c_{x\sigma}^\dagger, \quad (2.42)$$

$$c_{n\sigma} = \sum_x \psi_n^*(x) c_{x\sigma}. \quad (2.43)$$

These operators satisfy usual anti commutation relations (see the derivation in (A.4) and (A.5))

$$\{c_{n\sigma}, c_{m\tau}^\dagger\} = \delta_{nm} \delta_{\sigma\tau}, \quad (2.44)$$

$$\{c_{n\sigma}, c_{m\tau}\} = 0. \quad (2.45)$$

Thus, these operators are well behaved fermionic creation and annihilation operators. The number operators are given by:

$$n_{n\sigma} = c_{n\sigma}^\dagger c_{n\sigma} = W c_{x\sigma}^\dagger W^\dagger W c_{x\sigma} W^\dagger = W c_{x\sigma}^\dagger c_{x\sigma} W^\dagger = W n_{x\sigma} W^\dagger, \quad (2.46)$$

and can be written as:

$$n_{n\sigma} = \sum_{xx'} \psi_n(x) \psi_n^*(x') c_{x\sigma}^\dagger c_{x'\sigma}. \quad (2.47)$$

The inverse transformation in equations (2.40) and (2.41) is given by:

$$c_{x\sigma}^\dagger = W^\dagger c_{n\sigma}^\dagger W, \quad (2.48)$$

$$c_{x\sigma} = W^\dagger c_{n\sigma} W. \quad (2.49)$$

The spin operators keep the same form under this transformation (see the derivation in (A.6) and (A.7)).

$$S^z = \frac{1}{2} \sum_n (n_{n\uparrow} - n_{n\downarrow}). \quad (2.50)$$

$$S^+ = (S^-)^\dagger = \sum_n c_{n\uparrow}^\dagger c_{n\downarrow}. \quad (2.51)$$

Since W is unitary, the symmetries of the Hubbard Hamiltonian remain, but can be re-expressed using the new operators, namely

$$H_0 = \sum_{n\sigma} E_n c_{n\sigma}^\dagger c_{n\sigma}. \quad (2.52)$$

Next, we show that under a σ_3 transformation or particle-hole transformation H_0 becomes $-H_0$. Under a σ_3 transformation in (2.15), we obtain:

$$c_{n\sigma}^\dagger \rightarrow W_\sigma \epsilon(x) c_{x\sigma}^\dagger W_\sigma^\dagger. \quad (2.53)$$

We find that (see the derivation in (A.9)):

$$c_{n\sigma}^\dagger \rightarrow c_{-n\sigma}^\dagger, \quad (2.54)$$

$$c_{n\sigma} \rightarrow c_{-n\sigma}. \quad (2.55)$$

Under the transformation in (2.18), we have

$$c_{n\sigma}^\dagger \rightarrow W c_{x\sigma} W^\dagger = c_{n\sigma}, \quad (2.56)$$

$$c_{n\sigma} \rightarrow W c_{x\sigma}^\dagger W^\dagger = c_{n\sigma}^\dagger. \quad (2.57)$$

Under the transformation in (2.15), we have

$$H_0 \rightarrow \sum_{n\sigma} E_n c_{-n\sigma}^\dagger c_{-n\sigma} = - \sum_{n\sigma} E_{-n} c_{-n\sigma}^\dagger c_{-n\sigma} = - \sum_{n\sigma} E_n c_{n\sigma}^\dagger c_{n\sigma} = -H_0. \quad (2.58)$$

Under the transformation in (2.18), we have

$$H_0 \rightarrow \sum_{n\sigma} E_n c_{n\sigma} c_{n\sigma}^\dagger = \sum_{n\sigma} E_n (1 - c_{n\sigma}^\dagger c_{n\sigma}) = -H_0 + \sum_{n\sigma} E_n. \quad (2.59)$$

Since for every E_n there exists $E_{-n} = -E_n$, we obtain:

$$\sum_{n\sigma} E_n = 0, \quad (2.60)$$

so that $H_0 \rightarrow -H_0$. The interaction term can then be rewritten as

$$\begin{aligned} U &= u \sum_x n_{x\uparrow} n_{x\downarrow} = u \sum_x W^\dagger n_{n_x\uparrow} W W^\dagger n_{n_x\downarrow} W \\ &= u \sum_x \sum_{nmlk} \psi_n^*(x) \psi_l^*(x) \psi_m(x) \psi_k(x) c_{n\uparrow}^\dagger c_{m\uparrow} c_{l\downarrow}^\dagger c_{k\downarrow}. \end{aligned} \quad (2.61)$$

We note that this term conserves separately the number of spin up and spin down particles.

2.7 First order perturbation theory

To first order in perturbation theory we need to diagonalize the interaction term within the sub-space of the ground states. Then within this sub-space we obtain an effective Hamiltonian that takes into account only the zero modes. We introduce new notations $n_<, k_<$, which denote states with $E_n, E_k < 0$ and $\alpha, \beta, \gamma, \delta$ denotes the zero modes. We use the fact that we are in a subspace in which the negative energy levels are always occupied, so that

$$\begin{aligned} U &= u \sum_x n_{x\uparrow} n_{x\downarrow} = u \sum_x \sum_{n_< k_<} |\psi_n(x)|^2 |\psi_k(x)|^2 \\ &\quad + u \sum_x \sum_{n_< \alpha\beta} |\psi_n(x)|^2 \psi_\alpha^*(x) \psi_\beta(x) (c_{\alpha\uparrow}^\dagger c_{\beta\uparrow} + c_{\alpha\downarrow}^\dagger c_{\beta\downarrow}) \\ &\quad + u \sum_x \sum_{\alpha\beta\gamma\delta} \psi_\alpha^*(x) \psi_\beta^*(x) \psi_\gamma(x) \psi_\delta(x) c_{\alpha\uparrow}^\dagger c_{\beta\uparrow} c_{\gamma\downarrow}^\dagger c_{\delta\downarrow}. \end{aligned} \quad (2.62)$$

Note that the first term is constant and give the same contribution to all states while the other terms get a contribution only from the zero modes and hence exist because such zero modes exist on a bipartite lattice. Using the previous symmetries we can write an effective Hamiltonian (see the derivation in (A.15)):

$$H_{\text{eff}} = \frac{u}{2} \hat{N} + \frac{u}{2} \sum_{\alpha\beta\sigma} T_{\alpha\beta} c_{\alpha\sigma}^\dagger c_{\beta\sigma} + u \sum_{\alpha\beta\gamma\delta} V_{\alpha\beta\gamma\delta} c_{\alpha\uparrow}^\dagger c_{\beta\uparrow} c_{\gamma\downarrow}^\dagger c_{\delta\downarrow}, \quad (2.63)$$

where

$$\begin{aligned}
\hat{N} &= \sum_{\alpha} (n_{\alpha\uparrow} + n_{\alpha\downarrow}), \\
T_{\alpha\beta} &= - \sum_x \sum_{\gamma} |\psi_{\gamma}(x)|^2 \psi_{\alpha}^*(x) \psi_{\beta}(x), \\
V_{\alpha\beta\gamma\delta} &= \sum_x \psi_{\alpha}^*(x) \psi_{\beta}(x) \psi_{\gamma}^*(x) \psi_{\delta}(x),
\end{aligned} \tag{2.64}$$

with the symmetries:

$$\begin{aligned}
T_{\alpha\beta} &= T_{\beta\alpha}^*, \\
V_{\gamma\beta\alpha\delta} &= V_{\alpha\beta\gamma\delta}, \\
V_{\alpha\delta\gamma\beta} &= V_{\alpha\beta\gamma\delta}, \\
V_{\beta\alpha\delta\gamma} &= V_{\alpha\beta\gamma\delta}^*.
\end{aligned} \tag{2.65}$$

We also note that

$$T_{\alpha\beta} = - \sum_{\gamma} V_{\alpha\beta\gamma\gamma} \sum_{\alpha} T_{\alpha\alpha} = - \sum_{\alpha,\gamma} V_{\alpha\alpha\gamma\gamma}, \tag{2.66}$$

so that for a given number of vacancies and a given number of particles the energies can be written in terms of tensor elements of $V_{\alpha\beta\gamma\delta}$. We look for a maximal spin state, i.e. $S = \frac{|V_A - V_B|}{2}$ which we denote $|\psi\rangle$. Since all $|\psi\rangle$ s are degenerate, we can look for a state with all spins up and distributed on different zero modes (see example (2) in Fig. 2.3). This state satisfies:

$$\frac{2}{u} H_{\text{eff}} |\psi\rangle = \left(\hat{N} - \sum_{\alpha,\beta} V_{\alpha\alpha\beta\beta} \right) |\psi\rangle = (|V_A - V_B| + \text{Tr}(T)) |\psi\rangle. \tag{2.67}$$

Namely, a maximal spin state is an eigenstate of the effective Hamiltonian H_{eff} . We now add and subtract the maximal spin state energy:

$$\begin{aligned}
\frac{2}{u} H_{\text{eff}} &= \hat{N} + \sum_{\alpha\beta\sigma} T_{\alpha\beta} c_{\alpha\sigma}^{\dagger} c_{\beta\sigma} + 2 \sum_{\alpha\beta\gamma\delta} V_{\alpha\beta\gamma\delta} c_{\alpha\uparrow}^{\dagger} c_{\beta\uparrow} c_{\gamma\downarrow}^{\dagger} c_{\delta\downarrow} \\
&+ (|V_A - V_B| + \text{Tr}(T)) - (|V_A - V_B| + \text{Tr}(T)) \\
&\equiv H' + (|V_A - V_B| + \text{Tr}(T)),
\end{aligned} \tag{2.68}$$

so that in order to show that a maximal spin state is the ground state, we need to show that H' is positive semidefinite. We recall that a positive semidefinite operator is real and with non-negative eigenvalues. The ground state for such an operator has at least zero energy. If we find an eigenstate of a positive semidefinite operator with zero energy than it must be a ground state of that operator. For $N = |V_A - V_B|$ we have:

$$H' = \sum_{\alpha\beta\sigma} T_{\alpha\beta} c_{\alpha\sigma}^{\dagger} c_{\beta\sigma} + 2 \sum_{\alpha\beta\gamma\delta} V_{\alpha\beta\gamma\delta} c_{\alpha\uparrow}^{\dagger} c_{\beta\uparrow} c_{\gamma\downarrow}^{\dagger} c_{\delta\downarrow} - \text{Tr}(T). \tag{2.69}$$

Next, we define:

$$\begin{aligned}
A_\sigma(x) &= \sum_\alpha \psi_\alpha(x) c_{\alpha\sigma} \\
A_\sigma^\dagger(x) &= \sum_\alpha \psi_\alpha^*(x) c_{\alpha\sigma}^\dagger \\
C(x) &= \sum_\alpha |\psi_\alpha(x)|^2.
\end{aligned} \tag{2.70}$$

Note that:

$$\begin{aligned}
\{A_\sigma(x), A_\tau^\dagger(x)\} &= \sum_{\alpha,\beta} \psi_\alpha(x) \psi_\beta^*(x) \{c_{\alpha\sigma}, c_{\beta\tau}^\dagger\} \\
&= \sum_{\alpha,\beta} \psi_\alpha(x) \psi_\beta^*(x) \delta_{\alpha\beta} \delta_{\sigma\tau} \\
&= \sum_\alpha |\psi_\alpha(x)|^2 \delta_{\sigma\tau} \\
&= C(x) \delta_{\sigma\tau},
\end{aligned} \tag{2.71}$$

so that:

$$C(x) = A_\sigma(x) A_\sigma^\dagger(x) + A_\sigma^\dagger(x) A_\sigma(x). \tag{2.72}$$

Inserting these relations into (2.69) and using equation (2.64), we deduce:

$$H' = \sum_x \left(A_\uparrow^\dagger(x) A_\uparrow(x) A_\downarrow^\dagger(x) A_\downarrow(x) + A_\uparrow(x) A_\uparrow^\dagger(x) A_\downarrow(x) A_\downarrow^\dagger(x) \right). \tag{2.73}$$

Each term is clearly positive semidefinite so that H' is also positive semidefinite. Note that by definition:

$$A_\uparrow(x) = \sum_\alpha \psi_\alpha(x) c_{\alpha\uparrow} = \sum_{x'} \left(\sum_\alpha \psi_\alpha(x) \psi_\alpha^*(x') \right) c_{x'\uparrow}. \tag{2.74}$$

Hence, we conclude that to first order in perturbation theory in u/t , the ground state of the Hubbard Hamiltonian is non degenerate and it has a maximal spin. This result is very similar to Lieb's theorem (2.36). For example, in Fig. 2.3 example (2) is the true ground state of the system. The calculation we performed above using perturbation theory is very subtle for an infinite lattice. For a gap-less system it is difficult to define a zero mode subspace. Farther-more, there could be a quantum phase transition even for a small u , e.g., in a square lattice. However, we claim that the zero mode subspace is protected by the topology of the lattice and will be the only source for the spin in the ground state even for a gap less system. Another way to understand the validity of our result is to consider a translation invariant system as showed by [Mielke, 1993]. In that case the second term in 2.62 is constant and we obtain an effective Hubbard model in a subspace in which all the negative energy states are doubly occupied. The lowest energy state is degenerate $|V_A - V_B|$ times. [Mielke, 1993] has shown that for such Hubbard model the ground state is the one with maximal spin and it is non-degenerate, exactly as we obtained. Furthermore, the contribution to the total spin comes only from the

zero modes and so is the spin density. We see that by creating vacancies we can modify the spin of the ground state and obtain a ferromagnetic state if the number of vacancies is large enough. [Shen et al., 1994] defines the correlation function

$$m(0) = \frac{1}{N_{sites}} \langle S^+ S^- \rangle = \frac{1}{N_{sites}} \left\langle \left(\sum_x S_x^+ \right) \left(\sum_x S_x^- \right) \right\rangle. \quad (2.75)$$

By definition $S^+ S^-$ is a positive semidefinite operator. Note that $\langle S_i^+ S_j^- \rangle$ is positive (negative) if the ground state is symmetric (antisymmetric) with respect to i and j , i.e., the interaction between sites i and j is ferromagnetic (antiferromagnetic). This implies that if $m(0)$ is positive the system displays ferromagnetic long range order. Duplicating the calculation of [Shen et al., 1994] we obtain for a maximal spin state

$$m(0) = \frac{1}{4} \left(\frac{V_A}{N_{sites}} - \frac{V_B}{N_{sites}} \right)^2 N_{sites} + O(1). \quad (2.76)$$

The quantity $\left(\frac{V_A}{N_{sites}} - \frac{V_B}{N_{sites}} \right)^2$ could be finite implying $m(0) \propto N_{sites}$ and hence is extensive. We find that this system shows ferromagnetic long range order. If the number of vacancies is small there will not be long range order in the system, but there will still be long range correlation between distant vacancies.

2.8 Graphene as an example of a Hubbard model on a bipartite lattice - effect of vacancies

Graphene is faithfully described by a honeycomb lattice. In the tight binding approximation and nearest neighbor interaction, the physics of graphene is well accounted by a Hubbard model on a bipartite lattice. Recently theoretical ([Ovdat et al., 2018]) and experimental ([Ugeda et al., 2010]) work showed that upon creating vacancies, zero modes show up and are spatially localized on the vacancy sites (See Figs. 2.4 and 2.5).

Furthermore a local fractional charge is also formed around the vacancy (see Fig. 2.6). From our results, we find that a spin also shows up and it localized around the vacancies (see Fig. 2.7).

2.9 Entangled spin states

We found that the total spin in the ground state is $S = \frac{|V_A - V_B|}{2}$, and it has the expected $2S + 1$ degeneracy. While the states $|\uparrow\uparrow \cdots \uparrow\rangle$, $|\downarrow\downarrow \cdots \downarrow\rangle$ are separable states, the other states are entangled. Therefore the more vacancies we create, the more entangled states we can obtain.

In the example of graphene, this result implies that we can create spin entangled states on spatially distant vacancies (see Fig. 2.8).

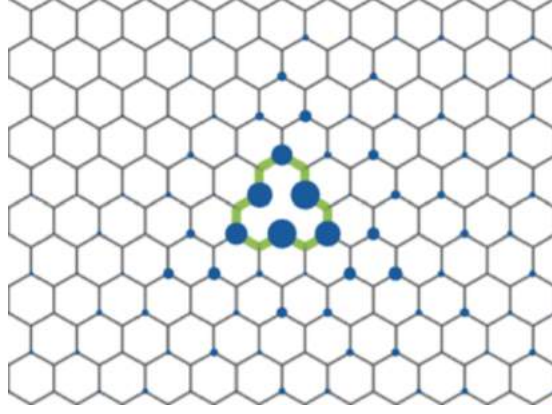


Figure 2.4: A spatially localized zero mode on a vacancy in graphene. The blue dots represent the strength of the square of the wave function of the zero modes (taken from [Ovdat et al., 2018]).

2.10 Connection to topology

We have found that the total spin in the ground state is $S = \frac{|V_A - V_B|}{2}$. Recall that $|V_A - V_B|$ is also the number of zero modes of H_0 and it is also the index of the Hamiltonian (equation (2.33)).

Therefore, the total spin in the ground state appears to be only a function of the number of vacancies, i.e., it is a property of the bipartite nature of the lattice and not its exact structure. We expect the spin to remain the same for a deformed yet bipartite lattice. In that sense the spin of the ground state is topologically protected. If the ground state is spin entangled, this property is expected to be protected by the topological nature of the zero modes. Another way to understand this statement is to consider the charge density at the ground state.

$$\rho(x) = \underbrace{\sum_n |\psi_n(x)|^2}_{\text{with vacancies}} - \underbrace{\sum_n |\psi_n(x)|^2}_{\text{no vacancies}}. \quad (2.77)$$

The total charge is $Q = \int dx \rho(x) = \frac{1}{2} \text{Index} H$, where the last equality is true for Graphene as shown by [Ovdat et al., 2018]. The Z component of spin density is

$$S_z(x) = \frac{1}{2} \left(\sum_{n\uparrow} |\psi_n(x)|^2 - \sum_{n\downarrow} |\psi_n(x)|^2 \right) \propto \rho(x)_\uparrow - \rho(x)_\downarrow. \quad (2.78)$$

The total Z component of the spin is

$$S_z = \int dx S_z(x) \propto Q_\uparrow - Q_\downarrow \propto \text{Index} H_\uparrow - \text{Index} H_\downarrow. \quad (2.79)$$

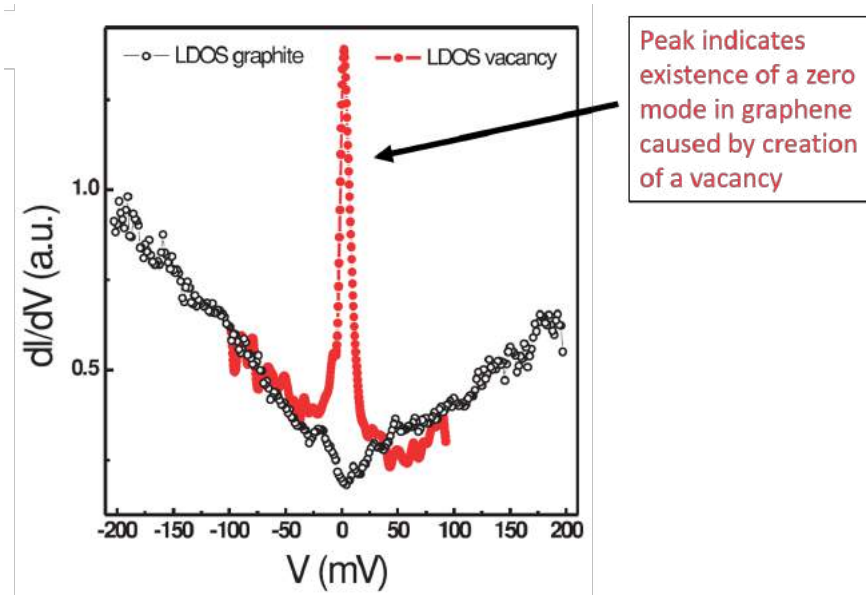


Figure 2.5: Measurement of the local density of states as a function of voltage (that can be converted to spectral energy) with and without vacancy. The sharp peak at zero energy (Fermi energy) corresponds to the expected zero mode localized on the vacancy (taken from [Ugeda et al., 2010], the figure was altered from the original).

A fully polarized state has

$$S = |S_z| \propto \text{Index}H_{\uparrow} \text{ or } \text{Index}H_{\downarrow}. \quad (2.80)$$

$SU(2)$ invariance of the spin implies that the spin in the ground state is only a function of the Index of the Hamiltonian for any polarization. The Index of the Hamiltonian is a topologically protected quantity and therefore so is the total spin. Graphene, thus appears to be a reliable setup to build and manipulate entangled spin states. Preliminary theoretical [Ovdat et al., 2018] and experimental [Mao et al., 2016] works give support to this proposal. Their work shows that the creation of vacancies results in localized zero modes on the vacancy sites.

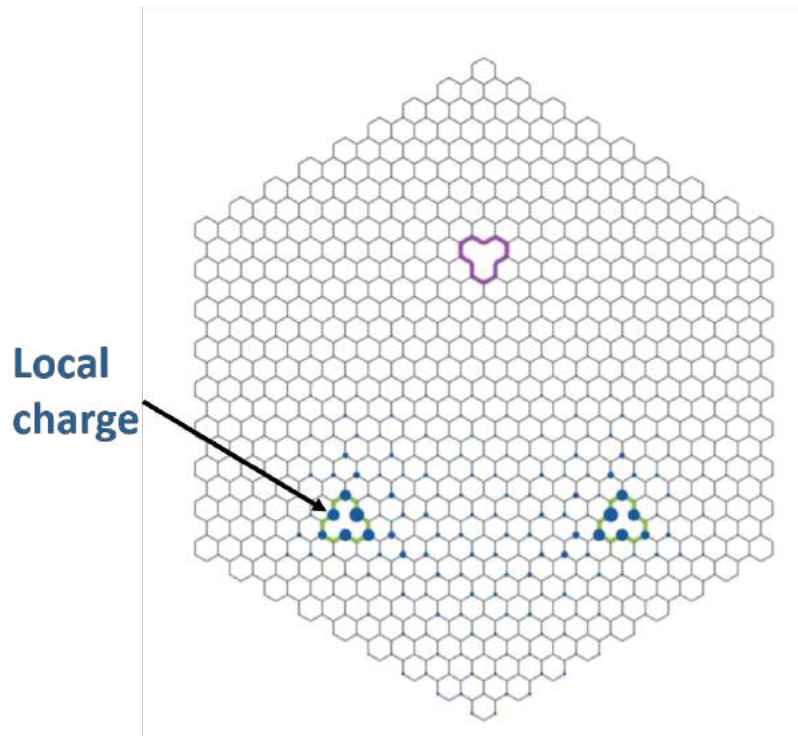


Figure 2.6: An example with two types of vacancies, each color (green or purple) represent a vacancy on a different sublattice. There are two green vacancies and one purple vacancy. A local fractional charge, which is proportional to zero mode wave function squared, (blue dots) is formed around the type of vacancies whose number is larger, in this case the green vacancies.

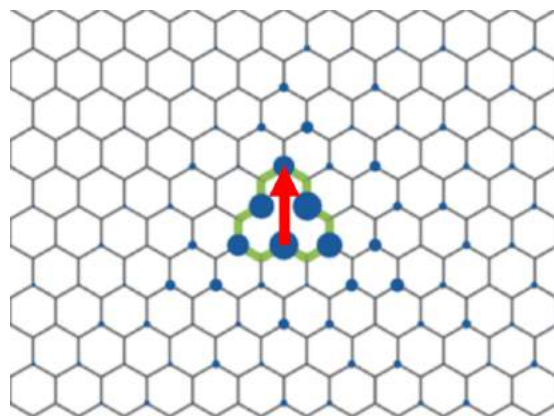


Figure 2.7: A spatially localized spin (blue dots) is formed around the vacancy. The red arrow represents the total spin in the z direction, which in this example is up.

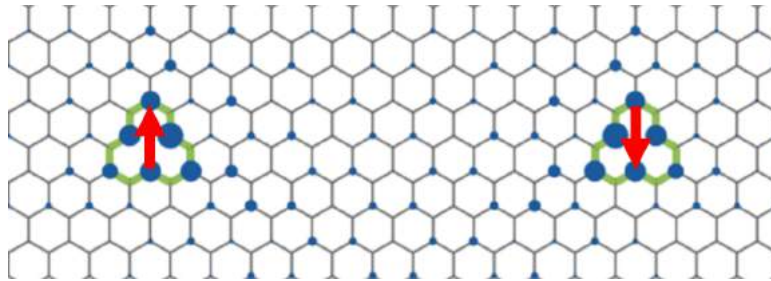


Figure 2.8: An example of a spin entangled state in graphene. The blue dots and red arrows are defined as in Fig. 2.7. In this example the total spin is $S = 1$ (from equation (2.36)), since there are two green vacancies and zero purple vacancies. Thus an entangled state $|\psi\rangle = \frac{1}{\sqrt{2}} (|\uparrow\downarrow\rangle + |\downarrow\uparrow\rangle)$ of two electrons on two distant vacancies can be created.

Chapter 3

Conclusion and open questions for fututre work

Bipartite lattices show simple yet very general properties. Their spectrum is symmetric and they have zero modes. We focused on the Hubbard model defined on a bipartite lattice. Following Lieb's theorem (2.30) for the spin of the ground state, we aimed to find the spin of the ground state for a bipartite lattice with a finite number of vacancies.

In Chapter 2 we discussed the properties and symmetries of the Hubbard model on a bipartite lattice with vacancies and used them to show that within perturbation theory, the spin of the ground state (2.36) is consistent with Lieb's theorem. We generalized this result for the case of vacancies and we were able to determine that the total spin and its spatial distribution are dependant only on the zero modes. We found that the spin spatial distribution is set by the subset of zero modes, and we gave a plausible argument for the existence of a topologically protected spin entangled states.

In a recent work [Ovdat et al., 2018] it has been shown that in graphene zero modes are spatially localized. We used that result to show how to build entangled spin states of electrons localized on distant vacancies.

Some questions remain unanswered. It is still an open question whether the total spin in the ground state is only a function of the number of vacancies to first order in perturbation theory, or is there some property that makes it generally true. We claim that the spin of the ground state is a topological feature of this system and therefore our result should hold to all orders in perturbation theory in u , but a proof is still required. We also plan to perform numerical calculation to support our claims. Another open problem is to understand how to create and manipulate the entanglement. Being able to control spatially remote entangled spins could prove useful in various applications such as quantum information. Moreover, the relevance of topological protection is reminiscent of similar features in other setups such as majorana fermions.

Appendix A

Appendix

A.1 Creation and annihilation operators transformations

A.1.1 Base transformation

The creation and annihilation operators transform as:

$$\begin{aligned} & c_{n_{k+1}\sigma_{k+1}}^\dagger |n_1, \sigma_1\rangle \otimes |n_2, \sigma_2\rangle \otimes \cdots \otimes |n_k, \sigma_k\rangle \\ &= |n_1, \sigma_1\rangle \otimes |n_2, \sigma_2\rangle \otimes \cdots \otimes |n_k, \sigma_k\rangle \otimes |n_{k+1}, \sigma_{k+1}\rangle \\ &= W |x_1, \sigma_1\rangle \otimes |x_2, \sigma_2\rangle \otimes \cdots \otimes |x_k, \sigma_k\rangle \otimes |x_{k+1}, \sigma_{k+1}\rangle \\ &= W c_{x_{k+1}\sigma_{k+1}}^\dagger |x_1, \sigma_1\rangle \otimes |x_2, \sigma_2\rangle \otimes \cdots \otimes |x_k, \sigma_k\rangle \\ &= W c_{x_{k+1}\sigma_{k+1}}^\dagger W^\dagger |n_1, \sigma_1\rangle \otimes |n_2, \sigma_2\rangle \otimes \cdots \otimes |n_k, \sigma_k\rangle. \end{aligned} \tag{A.1}$$

We conclude that:

$$c_{n\sigma}^\dagger = W c_{x\sigma}^\dagger W^\dagger, \tag{A.2}$$

$$c_{n\sigma} = W c_{x\sigma} W^\dagger. \tag{A.3}$$

These operators satisfy:

$$\begin{aligned} \{c_{n_x\sigma}, c_{n_y\tau}^\dagger\} &= \{W c_{x\sigma} W^\dagger, W c_{y\tau}^\dagger W^\dagger\} \\ &= W c_{x\sigma} W^\dagger W c_{y\tau}^\dagger W^\dagger + W c_{y\tau}^\dagger W^\dagger W c_{x\sigma} W^\dagger \\ &= W c_{x\sigma} c_{y\tau}^\dagger W^\dagger + W c_{y\tau}^\dagger c_{x\sigma} W^\dagger \\ &= W \{c_{x\sigma}, c_{y\tau}^\dagger\} W^\dagger \\ &= \delta_{xy} \delta_{\sigma\tau} W W^\dagger \\ &= \delta_{n_x n_y} \delta_{\sigma\tau}, \end{aligned} \tag{A.4}$$

$$\begin{aligned}
\{c_{n_x\sigma}, c_{n_y\tau}\} &= \{W c_{x\sigma} W^\dagger, W c_{y\sigma} W^\dagger\} \\
&= W \{c_{x\sigma}, c_{y\tau}\} W^\dagger \\
&= 0.
\end{aligned} \tag{A.5}$$

A.1.2 Spin operators

The spin operators transform as:

$$\begin{aligned}
S^z &= \frac{1}{2} \sum_x (n_{x\uparrow} - n_{x\downarrow}) \\
&= \frac{1}{2} \sum_x (W^\dagger n_{n_x\uparrow} W - W^\dagger n_{n_x\downarrow} W) \\
&= \frac{1}{2} \sum_x W^\dagger (n_{n_x\uparrow} - n_{n_x\downarrow}) W \\
&= \frac{1}{2} \sum_x \sum_{n_x n'_x} W_{x, n_x}^\dagger (n_{n_x\uparrow} - n_{n_x\downarrow}) W_{n'_x, x} \\
&= \frac{1}{2} \sum_{n_x n'_x} (n_{n_x\uparrow} - n_{n_x\downarrow}) \delta_{n_x, n'_x} \\
&= \frac{1}{2} \sum_{n_x} (n_{n_x\uparrow} - n_{n_x\downarrow}) \\
&= \frac{1}{2} \sum_n (n_{n\uparrow} - n_{n\downarrow}).
\end{aligned} \tag{A.6}$$

Similarly

$$S^+ = (S^-)^\dagger = \sum_n c_{n\uparrow}^\dagger c_{n\downarrow}. \tag{A.7}$$

A.1.3 Symmetries

Under σ_3 transformation (2.15) we have:

$$c_{n\sigma}^\dagger \rightarrow W_\sigma \epsilon(x) c_{x\sigma}^\dagger W_\sigma^\dagger. \tag{A.8}$$

To see what this operator is, we apply it on some state:

$$\begin{aligned}
&W_\sigma \epsilon(x) c_{x\sigma}^\dagger W_\sigma^\dagger |n_1, \sigma_1\rangle \otimes |n_2, \sigma_2\rangle \otimes \cdots \otimes |n_k, \sigma_k\rangle \\
&= W_\sigma \epsilon(x) c_{x\sigma}^\dagger |x_1, \sigma_1\rangle \otimes |x_2, \sigma_2\rangle \otimes \cdots \otimes |x_k, \sigma_k\rangle \\
&= W_\sigma \epsilon(x) |x_1, \sigma_1\rangle \otimes |x_2, \sigma_2\rangle \otimes \cdots \otimes |x_k, \sigma_k\rangle \otimes |x, \sigma\rangle \\
&= |n_1, \sigma_1\rangle \otimes |n_2, \sigma_2\rangle \otimes \cdots \otimes |n_k, \sigma_k\rangle W_\sigma \epsilon(x) |x, \sigma\rangle \\
&= |n_1, \sigma_1\rangle \otimes |n_2, \sigma_2\rangle \otimes \cdots \otimes |n_k, \sigma_k\rangle \sum_x \langle x, \sigma | n, \sigma \rangle \epsilon(x) |x, \sigma\rangle \\
&= |n_1, \sigma_1\rangle \otimes |n_2, \sigma_2\rangle \otimes \cdots \otimes |n_k, \sigma_k\rangle \otimes \sigma_3 |n, \sigma\rangle \\
&= |n_1, \sigma_1\rangle \otimes |n_2, \sigma_2\rangle \otimes \cdots \otimes |n_k, \sigma_k\rangle \otimes |-n, \sigma\rangle.
\end{aligned} \tag{A.9}$$

We conclude that:

$$c_{n\sigma}^\dagger \rightarrow c_{-n\sigma}^\dagger, \quad (\text{A.10})$$

$$c_{n\sigma} \rightarrow c_{-n\sigma}. \quad (\text{A.11})$$

A.2 The effective Hamiltonian

We obtain an effective Hamiltonian from equation (2.62). For the second term we can use the fact that

$$\delta_{xx} = \sum_i |\psi_i(x)|^2, \quad (\text{A.12})$$

where i runs over all states. Since the unperturbed Hamiltonian has a symmetry of positive and negative energy's this can be written as

$$\delta_{xx} = 2 \sum_{n<} |\psi_n(x)|^2 + \sum_{\alpha} |\psi_{\alpha}(x)|^2. \quad (\text{A.13})$$

Therefore we get:

$$\sum_{n<} |\psi_n(x)|^2 = \frac{\delta_{xx} - \sum_{\alpha} |\psi_{\alpha}(x)|^2}{2}. \quad (\text{A.14})$$

Effectively we can write:

$$\begin{aligned} H_{\text{eff}} &= u \sum_x \sum_{\alpha\beta} \frac{\delta_{xx} - \sum_{\gamma} |\psi_{\gamma}(x)|^2}{2} \psi_{\alpha}^*(x) \psi_{\beta}(x) \left(c_{\alpha\uparrow}^\dagger c_{\beta\uparrow} + c_{\alpha\downarrow}^\dagger c_{\beta\downarrow} \right) \\ &+ u \sum_x \sum_{\alpha\beta\gamma\delta} \psi_{\alpha}^*(x) \psi_{\beta}(x) \psi_{\gamma}^*(x) \psi_{\delta}(x) c_{\alpha\uparrow}^\dagger c_{\beta\uparrow} c_{\gamma\downarrow}^\dagger c_{\delta\downarrow} \\ &= \frac{u}{2} N + \frac{u}{2} \sum_{\alpha\beta\sigma} T_{\alpha\beta} c_{\alpha\sigma}^\dagger c_{\beta\sigma} + u \sum_{\alpha\beta\gamma\delta} V_{\alpha\beta\gamma\delta} c_{\alpha\uparrow}^\dagger c_{\beta\uparrow} c_{\gamma\downarrow}^\dagger c_{\delta\downarrow}, \end{aligned} \quad (\text{A.15})$$

where

$$\begin{aligned} N &= \sum_{\alpha} (n_{\alpha\uparrow} + n_{\alpha\downarrow}) \\ T_{\alpha\beta} &= - \sum_x \sum_{\gamma} |\psi_{\gamma}(x)|^2 \psi_{\alpha}^*(x) \psi_{\beta}(x) \\ V_{\alpha\beta\gamma\delta} &= \sum_x \psi_{\alpha}^*(x) \psi_{\beta}(x) \psi_{\gamma}^*(x) \psi_{\delta}(x). \end{aligned} \quad (\text{A.16})$$

Plugging equations (2.64) , (2.70) and (2.71) into equation (2.69) we get:

$$\begin{aligned}
H' &= \sum_{\alpha\beta\sigma} T_{\alpha\beta} c_{\alpha\sigma}^\dagger c_{\beta\sigma} + 2 \sum_{\alpha\beta\gamma\delta} V_{\alpha\beta\gamma\delta} c_{\alpha\uparrow}^\dagger c_{\beta\uparrow} c_{\gamma\downarrow}^\dagger c_{\delta\downarrow} - \text{Tr}(T) \\
&= \sum_x \left(- \sum_{\alpha\beta\gamma\sigma} |\psi_\gamma(x)|^2 \psi_\alpha^*(x) \psi_\beta(x) c_{\alpha\sigma}^\dagger c_{\beta\sigma} \right) \\
&+ \sum_x \left(2 \sum_{\alpha\beta\gamma\delta} \psi_\alpha^*(x) \psi_\beta(x) \psi_\gamma^*(x) \psi_\delta(x) c_{\alpha\uparrow}^\dagger c_{\beta\uparrow} c_{\gamma\downarrow}^\dagger c_{\delta\downarrow} \right) \\
&+ \sum_x \left(\sum_{\alpha\beta} |\psi_\alpha(x)|^2 |\psi_\beta(x)|^2 \right) \\
&= \sum_x \left(-C(x) \sum_\sigma A_\sigma^\dagger(x) A_\sigma(x) + 2A_\uparrow^\dagger(x) A_\uparrow(x) A_\downarrow^\dagger(x) A_\downarrow(x) + C^2(x) \right) \\
&= \sum_x \left(-C(x) \left(A_\uparrow^\dagger(x) A_\uparrow(x) + A_\downarrow^\dagger(x) A_\downarrow(x) \right) \right) \\
&+ \sum_x \left(2A_\uparrow^\dagger(x) A_\uparrow(x) A_\downarrow^\dagger(x) A_\downarrow(x) + C^2(x) \right).
\end{aligned} \tag{A.17}$$

In the first term we use:

$$C(x) = A_\downarrow(x) A_\downarrow^\dagger(x) + A_\downarrow^\dagger(x) A_\downarrow(x), \tag{A.18}$$

in the second term we use:

$$C(x) = A_\uparrow(x) A_\uparrow^\dagger(x) + A_\uparrow^\dagger(x) A_\uparrow(x), \tag{A.19}$$

and in the last term we use one of each, so that we can write:

$$\begin{aligned}
H' &= \sum_x \left(-C(x) \left(A_\uparrow^\dagger(x) A_\uparrow(x) + A_\downarrow^\dagger(x) A_\downarrow(x) \right) \right) \\
&+ \sum_x \left(2A_\uparrow^\dagger(x) A_\uparrow(x) A_\downarrow^\dagger(x) A_\downarrow(x) + C^2(x) \right) \\
&= - \sum_x \left(A_\downarrow(x) A_\downarrow^\dagger(x) A_\uparrow^\dagger(x) A_\uparrow(x) + A_\downarrow^\dagger(x) A_\downarrow(x) A_\uparrow^\dagger(x) A_\uparrow(x) \right) \\
&- \sum_x \left(A_\uparrow(x) A_\uparrow^\dagger(x) A_\downarrow^\dagger(x) A_\downarrow(x) + A_\uparrow^\dagger(x) A_\uparrow(x) A_\downarrow^\dagger(x) A_\downarrow(x) \right) \\
&+ \sum_x \left(2A_\uparrow^\dagger(x) A_\uparrow(x) A_\downarrow^\dagger(x) A_\downarrow(x) \right) \\
&+ \sum_x \left(\left(A_\uparrow(x) A_\uparrow^\dagger(x) + A_\uparrow^\dagger(x) A_\uparrow(x) \right) \left(A_\downarrow(x) A_\downarrow^\dagger(x) + A_\downarrow^\dagger(x) A_\downarrow(x) \right) \right) \\
&= \sum_x \left(A_\uparrow^\dagger(x) A_\uparrow(x) A_\downarrow^\dagger(x) A_\downarrow(x) + A_\uparrow(x) A_\uparrow^\dagger(x) A_\downarrow(x) A_\downarrow^\dagger(x) \right)
\end{aligned} \tag{A.20}$$

Bibliography

- [Anderson, 1959] Anderson, P. W. (1959). New Approach to the Theory of Superexchange Interactions. *Physical Review*, 115(1):2–13.
- [Brouwer et al., 2002] Brouwer, P. W., Racine, E., Furusaki, A., Hatsugai, Y., Morita, Y., and Mudry, C. (2002). Zero modes in the random hopping model. *Physical review B*, 66(1):014204.
- [Charlebois et al., 2015] Charlebois, M., Sénéchal, D., Gagnon, A. M., and Tremblay, A. M. S. (2015). Impurity-induced magnetic moments on the graphene-lattice Hubbard model: An inhomogeneous cluster dynamical mean-field theory study. *Physical review B*, 91(3):035132.
- [González-Herrero et al., 2016] González-Herrero, H., Gómez-Rodríguez, J. M., Mallet, P., Moaied, M., Palacios, J. J., Salgado, C., Ugeda, M. M., Veuillen, J.-Y., Yndurain, F., and Brihuega, I. (2016). Atomic-scale control of graphene magnetism by using hydrogen atoms. *Science*, 352(6284):437–441.
- [Hatsugai et al., 2015] Hatsugai, Y., Shiraishi, K., and Aoki, H. (2015). Flat bands in the Weaire-Thorpe model and silicene. *New Journal of Physics*, 17(2):025009.
- [Iadecola et al., 2016] Iadecola, T., Schuster, T., and Chamon, C. (2016). Non-Abelian Braiding of Light. *Physical Review Letters*, 117(7):073901.
- [Kindermann, 2009] Kindermann, M. (2009). Pseudospin entanglement and Bell test in graphene. *Physical review B*, 79(11):115444.
- [Lieb and Mattis, 1962a] Lieb, E. and Mattis, D. (1962a). Ordering Energy Levels of Interacting Spin Systems. *Journal of Mathematical Physics*, 3(4):749–751.
- [Lieb and Mattis, 1962b] Lieb, E. and Mattis, D. (1962b). Theory of Ferromagnetism and the Ordering of Electronic Energy Levels. *Physical Review*, 125(1):164–172.
- [Lieb, 1989] Lieb, E. H. (1989). Two theorems on the Hubbard model. *Physical Review Letters*, 62(10):1201–1204.

- [Liu et al., 2015] Liu, Y., Weinert, M., and Li, L. (2015). Determining charge state of graphene vacancy by noncontact atomic force microscopy and first-principles calculations. *Nanotechnology*, 26(3):035702.
- [Mao et al., 2016] Mao, J., Jiang, Y., Moldovan, D., Li, G., Watanabe, K., Taniguchi, T., Masir, M. R., Peeters, F. M., and Andrei, E. Y. (2016). Realization of a tunable artificial atom at a supercritically charged vacancy in graphene. *Nature Physics*, 12(6):545–549.
- [Mielke, 1991a] Mielke, A. (1991a). Ferromagnetic ground states for the Hubbard model on line graphs. *Journal of Physics A Mathematical General*, 24(2):L73–L77.
- [Mielke, 1991b] Mielke, A. (1991b). Ferromagnetism in the Hubbard model on line graphs and further considerations. *Journal of Physics A Mathematical General*, 24(14):3311–3321.
- [Mielke, 1992] Mielke, A. (1992). Exact ground states for the Hubbard model on the Kagome lattice. *Journal of Physics A Mathematical General*, 25(16):4335–4345.
- [Mielke, 1993] Mielke, A. (1993). Ferromagnetism in the Hubbard model and Hund’s rule. *Physics Letters A*, 174(5-6):443–448.
- [Mielke and Tasaki, 1993] Mielke, A. and Tasaki, H. (1993). Ferromagnetism in the Hubbard model: Examples from models with degenerate single-electron ground states. *Communications in Mathematical Physics*, 158(2):341–371.
- [Nagaoka, 1966] Nagaoka, Y. (1966). Ferromagnetism in a Narrow, Almost Half-Filled s Band. *Physical Review*, 147(1):392–405.
- [Nanda et al., 2012] Nanda, B. R. K., Sherafati, M., Popović, Z. S., and Satpathy, S. (2012). Electronic structure of the substitutional vacancy in graphene: density-functional and Green’s function studies. *New Journal of Physics*, 14(8):083004.
- [Ovdat et al., 2018] Ovdat, O., Don, Y., and Akkermans, E. (2018). Vacancies in Graphene : Dirac Physics and Fractional Vacuum Charges. *arXiv e-prints*, page arXiv:1807.10297.
- [Palacios et al., 2008] Palacios, J. J., Fernández-Rossier, J., and Brey, L. (2008). Vacancy-induced magnetism in graphene and graphene ribbons. *Physical review B*, 77(19):195428.
- [Pereira et al., 2007] Pereira, V. M., Guinea, F., Lopes Dos Santos, J. M. B., Peres, N. M. R., and Castro Neto, A. H. (2007). Erratum: Disorder Induced Localized States in Graphene [Phys. Rev. Lett. 96, 036801 (2006)]. *Physical Review Letters*, 98(25):259902.

- [Shen et al., 1994] Shen, S.-Q., Qiu, Z.-M., and Tian, G.-S. (1994). Ferrimagnetic long-range order of the Hubbard model. *Physical Review Letters*, 72(8):1280–1282.
- [Sutherland, 1986] Sutherland, B. (1986). Localization of electronic wave functions due to local topology. *Physical review B*, 34(8):5208–5211.
- [Ugeda et al., 2010] Ugeda, M. M., Brihuega, I., Guinea, F., and Gómez-Rodríguez, J. M. (2010). Missing Atom as a Source of Carbon Magnetism. *Physical Review Letters*, 104(9):096804.
- [Ulybyshev and Katsnelson, 2015] Ulybyshev, M. V. and Katsnelson, M. I. (2015). Magnetism and Interaction-Induced Gap Opening in Graphene with Vacancies or Hydrogen Adatoms: Quantum Monte Carlo Study. *Physical Review Letters*, 114(24):246801.
- [Vogt et al., 2012] Vogt, P., De Padova, P., Quaresima, C., Avila, J., Frantzeskakis, E., Asensio, M. C., Resta, A., Ealet, B., and Le Lay, G. (2012). Silicene: Compelling Experimental Evidence for Graphenelike Two-Dimensional Silicon. *Physical Review Letters*, 108(15):155501.
- [Yazyev and Helm, 2007] Yazyev, O. V. and Helm, L. (2007). Defect-induced magnetism in graphene. *Physical review B*, 75(12):125408.

מצבים שזורים של ספינים הנמצאים במיקום של האטומים החסרים המרוחקים אחד מהשני מרחבית. חלק מהשאלות הינן עדיין בגדר תעלומה. אחת מהשאלות הפתוחות היא האם הספין הכולל במצב היסוד הוא רק פונקציה של מספר האטומים החסרים בסדר ראשון בתורת הפרעות, או האם ישנה תכונה המחייבת את התוצאה הזו להיות נכונה במדויק. אנו מניחים כי הספין במצב היסוד הוא תכונה טופולוגית של המערכת הזו ולכן התוצאה שלנו צריכה להיות נכונה בכל סדר בתורת הפרעות באינטראקציית האברד, אך עדיין חסרה ההוכחה. בעיה פתוחה נוספת הינה כיצד ניתן לייצר ולהשפיע על השזירות. היכולת לשלוט בספינים שזורים המרוחקים אחד מהשני יכולה להיות מאוד שימושית בתחומים שונים, למשל באינפורמציה קוונטית. בנוסף הרלוונטיות של הגנה טופולוגית מזכירה תכונות דומות במערכות נוספות, כגון פרמיוני מיורנה.

תקציר

תזה זו מוקדשת למחקר של הספין הכולל במצב היסוד של פרמיונים בעלי ספין חצי, באמצעות מודל האברד המוגדר על סריגים דו חלקיים עם אטומים בודדים חסרים. סריגים דו חלקיים מוגדרים כסכום ישר של שני תתי סריגים A ו-B, כך שכל אתר מחובר לאתרים השייכים לתת הסריג השני. הספקטרום של המילטוניאנים חד חלקיקיים על סריגים כאלו הינו בעל סימטריה של אנרגיות חיוביות ושיליות ויכולים להיות לו מצבים עם אפס אנרגיה. מספר המצבים בעלי אפס אנרגיה יכול להיות מסדר גודל של מספר האתרים בסריג, כלומר מקרוסקופי. אטום בודד חסר מוגדר על ידי הסרה של אתר סריג אחד מתת סריג A או B מבלי לפגוע במבנה הדו חלקי של הסריג. תוצאה חשובה של ליב (1989) קובעת את הספין במצב היסוד של מודל האברד עם אינטראקציית דחיה על סריגים דו חלקיים עם מספר סופי של אתרים, ללא אטומים בודדים חסרים, לכל אינטראקציית האברד.

על ידי שימוש בסדר ראשון בתורת הפרעות, כלומר אינטראקציית חלשה בין פרמיונים באותו אתר, מצאנו כי בנוכחות מספר סופי של אטומים בודדים חסרים V_A ו- V_B למצב היסוד יש ספין סופי הנתון על ידי $S = \frac{1}{2}|V_A - V_B|$. תוצאה זו בלתי תלויה במספר אתרי הסריג (סופי או אינסופי), במימד הסריג או במבנה המדויק שלו, והיא נובעת ממצבים בעלי אפס אנרגיה הנוצרים מהאטומים הבודדים החסרים. אנו מציגים הסבר הגיוני לכך שניתן לעבוד עם סריג דו חלקי אינסופי כאשר מספר האתרים בכל אחד מתתי הסריגים מוחלף במספר האטומים החסרים בכל אחד מהם ובכך מכלילים את התוצאה של ליב לסריגים אינסופיים עם אטומים בודדים חסרים. המצבים בעלי אפס אנרגיה מגדירים תת מרחב למרחב ההילברט המלא שנשאר אינווריאנטי תחת אינטראקציית האברד. החוזק של תוצאה זו נובע מתכונות טופולוגיות של סריגים דו חלקיים שלא נצפו בספרות. אנו משתמשים בכך שהספין במצב היסוד מוגן טופולוגית; אנו מניחים שהתוצאה שלנו נכונה גם מעבר לתורת הפרעות, וצופים שלספינים השזורים יש תכונות מעניינות. גרפן הינו מערכת דו מימדית של אטומי פחמן המסודרים במבנה של חלת דבש. במסגרת קירוב של אינטראקציות בין שכנים קרובים, סריג הגרפן הוא סריג דו חלקי ולכן הוא מהווה פלטפורמה טבעית לרעיונות שהצגנו ויכול להיות בסיס לשימושים מעניינים עבורם. לאחרונה התגלה כי המצבים בעלי אפס אנרגיה בגרפן ממוקמים מרחבית. בנוסף, מספר המצבים בעלי אפס אנרגיה בגרפן הוא האינדקס של ההמילטוניאן המתאר את הגרפן בגבול של אנרגיות נמוכות. אינדקס זה מקיים את תנאי משפט האינדקס של עטיה וזינגר, לכן הוא אינדקס טופולוגי, ולכן הספין במצב היסוד של מודל האברד בגרפן גם הוא צפוי להיות גודל טופולוגי. אנו משתמשים בתוצאה זו כדי להראות שניתן לבנות בעזרת גרפן

המחקר בוצע בהנחייתו של פרופסור אריק אקרמן בפקולטה לפיזיקה.

תודות

ברצוני להודות למנחה שלי פרופ' אריק אקרמן על התמיכה שלו לאורך המחקר וכתירת התזה שלי, עבור ההערות המצוינות שלו על העבודה שלי, ועבור הרבה פגישות קבוצה מרתקות ושיחות מעניינות בזמן ארוחות צהריים.

אני מודה לטכניון על התמיכה הכספית הנדיבה בהשתלמותי.

מודל האברד על סריג דו חלקי: מצבים בעלי אנרגיה אפס ומצבי ספין שזורים

חיבור על מחקר

לשם מילוי חלקי של הדרישות לקבלת התואר
מגיסטר למדעים בפיזיקה

עמית גופט

הוגש לסנט הטכניון --- מכון טכנולוגי לישראל
ניסן התש"פ חיפה אפריל 2020

**מודל האברד על סריג דו חלקי:
מצבים בעלי אנרגיה אפס ומצבי ספין
שזורים**

עמית גופט